Atomistic mechanisms for chemical defects formation in polyethylene

Lihua Chen, Huan Doan Tran 🆔 , and Rampi Ramprasad

ARTICLES YOU MAY BE INTERESTED IN

Atomistic mechanisms for chemical defects formation in polyethylene

Lihua Chen,[1] Huan Doan Tran,[1,2,a)] and Rampi Ramprasad[1]

[1]*School of Materials Science and Engineering, Georgia Institute of Technology, 771 Ferst Drive NW, Atlanta, Georgia 30332, USA*
[2]*Department of Materials Science and Engineering, University of Connecticut, 97 North Eagleville Road, Storrs, Connecticut 06269, USA*

Chemical defects can progressively degrade the electronic structure of polymer dielectrics, ultimately leading to their failure. Because the polymer degradation and breakdown related processes are notably complicated in nature, they remain far from being understood both experimentally and computationally. Using a combination of density functional theory calculations and classical molecular dynamics simulations, we propose seven atomistic mechanisms for the formation of common chemical defects in polyethylene using which a variety of defect-related experimental observations can be explained. This work provides a comprehensive connection among the experiments related to polyethylene defects and aging, laying the groundwork for an understanding of polymer degradation and breakdown. *Published by AIP Publishing.* https://doi.org/10.1063/1.5063944

I. INTRODUCTION

Polymers, e.g., polyethylene (PE) and polypropylene, are widely used as dielectric materials in electronic and electric devices.[1,2] Under operation conditions, chemical defects are progressively introduced in the polymers,[3] degrading their electronic structure,[4–6] and initiating and facilitating undesired carrier transport.[7] Sufficiently high-energy, or "hot," carriers could either self-multiply or catalyze the creation of new defects. These processes, which may eventually lead to the breakdown of the polymers, span over enormous time and length scales, thus posing major challenges for both experimental and computational investigations.[1,2,6,8–11]

In fact, most past modeling efforts on polymer degradation are limited to exploring possible chemical defects, primarily by using (static) calculations to assess their energetic favorability.[4–6] A past first-principles molecular dynamics (MD) study provided initial insights on factors that could contribute to the formation of chemical defects in PE.[3] Among electrons, holes, and excitons already present in the system (e.g., due to field-induced charge injection), it was found that triplet excitons localizing in a distorted region of PE could weaken the C–H bonds nearby, facilitating bond scission and forming PE-CH* radicals, i.e., PE $\rightarrow$ PE-$(CH^*)_2$ + H_2. When there are two (intra-chain) adjacent PE-CH* radicals, the excitons trapped between them may then recombine radiatively to form a vinyl (CH=CH) defect. The computed wavelength of the radiated photon is ≃400–412-nm, being consistent with available phosphorescence measurements.[12]

The PE-CH* radical, from which vinyl defects can be formed,[3] is likely the starting point for the formation of a sequence of PE chemical defects whose configurations and identities are defined in Fig. 1(a). By exposing PE samples that contain vinyl defects to air, water, light and heat, a large number of photooxidation and thermal oxidation products, e.g., PE-COOH, PE-C=O, PE-OH, and PE-HC=O, have been proposed to form and observed experimentally.[10,13–21] Such oxidation-related defects are known[22] to play an important role in polymer degradation and breakdown, presumably via triggering the charge transport as experimentally observed in some polymers.[7]

The goal of this paper is to computationally explore the oxidation-induced chemical defects of PE and systematically fill the gap of the current understanding of polymer degradation. Using a combination of density functional theory (DFT) calculations and classical force-field based MD simulations, we propose seven mechanisms for PE chemical defect creation, labeled M1-M7, which are summarized in Fig. 1. Starting from the formation of PE-CH* (M1),[3] two mechanisms M2 and M3 follow, creating either PE-CH=CH (vinyl) or PE-COOH (hydroperoxide). In the latter case, PE-COOH can be decomposed into either PE-C=O (M4) or PE-CO* (M5) by reacting with an intra- or inter-molecule H atom, respectively. Finally, mechanisms M6 and M7 lead to the formation of PE-HC=O or PE-OH. The proposed mechanisms leading to these defects are validated in multiple ways. Experimental observations of PE-COOH[16] and PE-HC=O[17,18] and/or the measurements of appropriate bond dissociation energy[23] and luminescence energy[12] support the proposed mechanisms of PE chemical defects formation. Our findings have provided a comprehensive connection among the available experiments related to PE defects and laid the groundwork for an understanding of polymer degradation and breakdown.

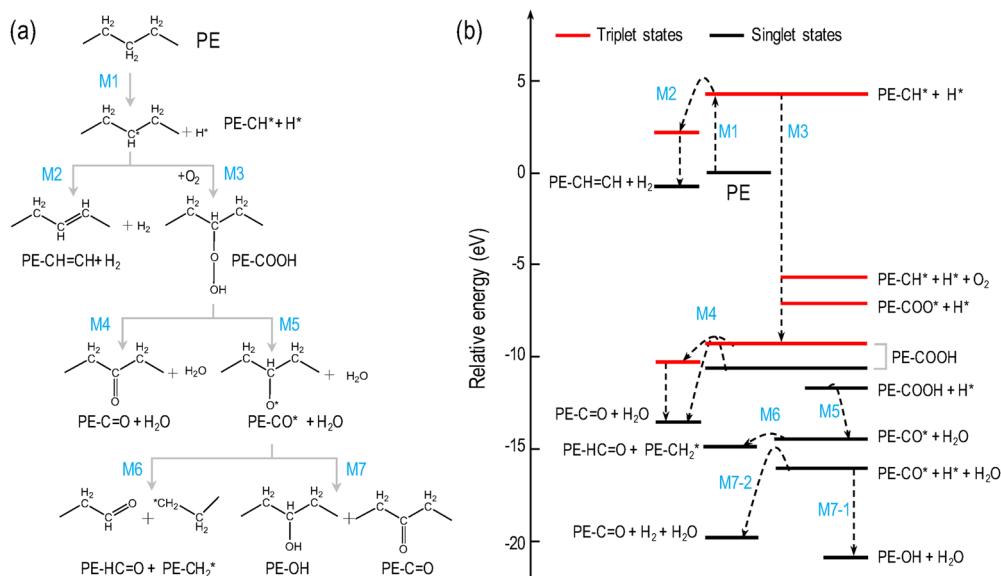a)Electronic mail: huan.tran@mse.gatech.edu

FIG. 1. (a) Chemical defect formation mechanisms (M1-M7) of PE and (b) DFT relative energies associated with M1-M7, given with respect to the energy of the singlet PE. The species at triplet and singlet states are shown in red and black, respectively.

II. COMPUTATIONAL METHODS

Our model contains an isolated (*all-trans*) single PE chain of 10 CH_2 units, surrounded by at least 15 Å of vacuum. This model was constructed to reliably capture the defect formation mechanisms while being computationally affordable with our numerical scheme. Each reaction involves a chemical defect of a CH_2 unit and some hydrogen atoms nearby. For a carbon atom in the PE crystal structure optimized by DFT,[24] the closest hydrogen atoms are from the adjacent (intra-chain) CH_2 units, which are at the distance of $\simeq 2.2$ Å. On the other hand, any inter-chain hydrogen atom is at least $\simeq 3.4$ Å away. Therefore, the proposed reactions would likely involve the intra-chain hydrogen atoms.

The numerical scheme used for this work was designed to adequately describe both static and dynamic characteristics of the proposed reactions. The dynamics of the reactions

were probed via MD simulations, performed using *Large-scale Atomic/Molecular Massively Parallel Simulator* (LAMMPS)[25] and employing the reactive force field (ReaxFF).[26,27] In the NVT MD simulations (of M3, M5, M6, and M7), which extend to 100 ps with a time step of 0.1 fs, we used the reactant structures optimized by DFT. For M3, M5, and M7, the temperature T was set to 300 K, while for M6, T was increased to 1000 K for the reaction to happen. Reasonable reaction probabilities were also ensured by using 3 oxygen molecules (O_2) and 5 hydrogen radicals (H^*) in the model. The static characteristics of the proposed reactions were captured by calculations using the climbing-image nudge elastic band (CINEB) method.[28] The CINEB algorithms were coupled with Γ−point DFT calculations, performed using the *Vienna Ab initio simulation package* (VASP).[29–31] Our calculations employed the Perdew-Burke-Ernzerhof exchange-correlation functional[32] and a plane-wave energy cutoff of 400 eV. The
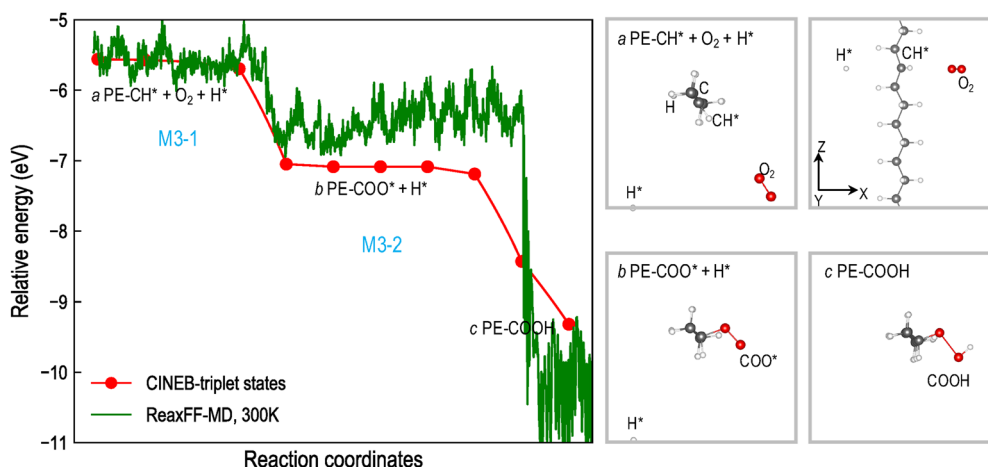

FIG. 2. (Left) CINEB reaction path (red) and ReaxFF-MD trajectories at 300 K (green) of mechanism M3 and (right) the structure of reactants, transition states, and products. Relative energy is given with respect to that of singlet PE.
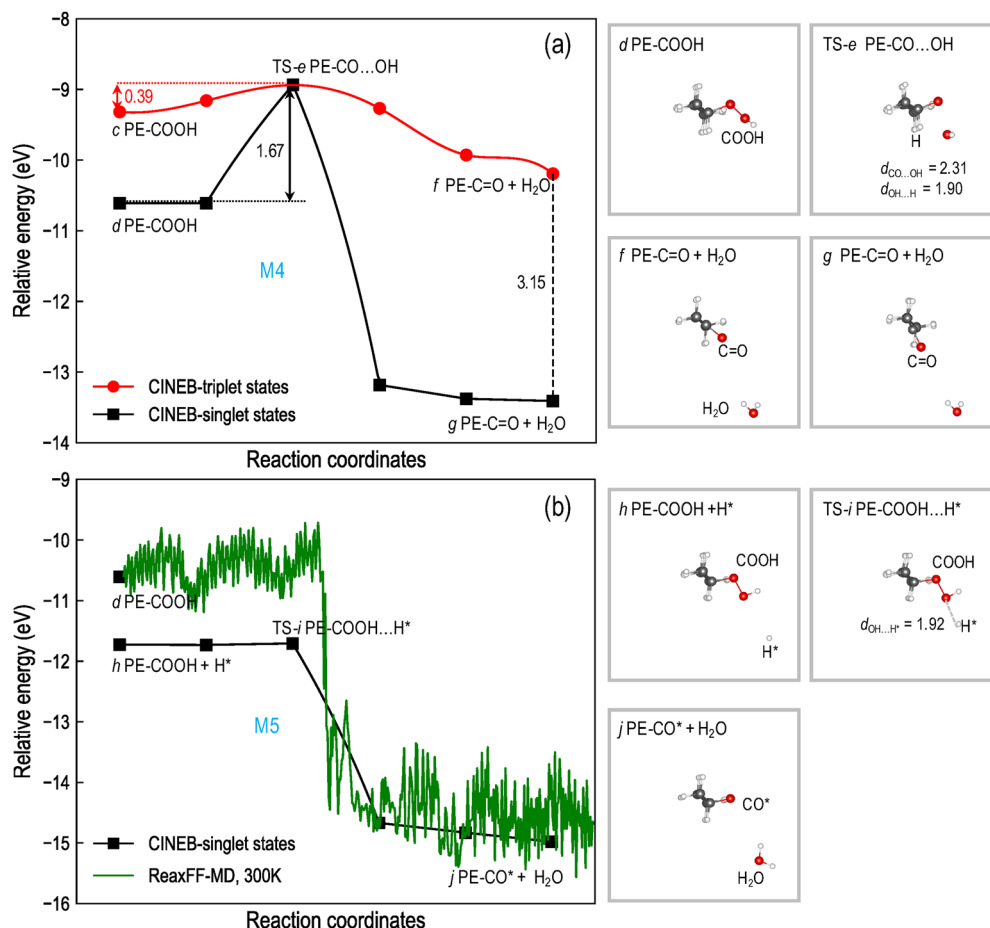
FIG. 3. (Left) CINEB reaction pathways (singlet in black and triplet in red) and ReaxFF-MD trajectory at 300 K (green) of M4 (a) and M5 (b), and (right) the structures of reactants, transition states, and products of mechanisms M4 (a) and M5 (b).

vibrational free energy is neglected because such small terms tend to cancel out when relative energies like energy barriers or reaction energies are calculated, while computing them is very time-consuming for our model. Moreover, the (interchain) van der Waals (vdW) interactions do not appear in the single-chain model, and thus they were not considered. Except for the exclusion of the vdW interactions, this scheme is reasonable for calculating energy-related properties of polymers, according to Ref. 24.

The ReaxFF-based MD and DFT computational methods are different in the level of theory. Therefore, the agreement between the results from these methods, as shown in Figs. 2–4, is expected to be qualitative, i.e., the proposed reaction mechanisms should be consistent, rather than quantitative, i.e., the energy barrier may be somewhat different. Given that MD simulations were performed at 300 K and 1000 K while the DFT-based calculations were limited at 0 K, entropic effects can also contribute to the differences.

III. RESULTS AND DISCUSSIONS

A. M1: PE → PE-CH* + H*

The formation of PE-CH* radicals, according to PE-CH$_2$ (ground) → PE-CH$_2$ (triplet) → PE-CH* + H* (singlet), was proposed by Bealing and Ramprasad.[3] In this

mechanism, PE is assumed to be in its excited triplet state, which may be created by heat, ultraviolet (UV) irradiation, or external electric field.[16,33,34] The excitons trapped within distorted regions of PE could then weaken and break the C–H bonds nearby, forming the PE-CH* radicals. The estimated barrier of this pathway is very small (0.025 eV, being comparable to the room-temperature thermal energy), suggesting that PE-CH* radicals are likely formed via this mechanism.[3] In this paper, mechanism M1 is proposed to be the starting point of a chain of PE oxidation-induced defects, which may be responsible for degradation of PE under working conditions.

B. M2 and M3: PE-CH=CH and PE-COOH formation

Starting from the resulted PE-CH* radicals, two mechanisms M2 and M3 can follow, creating either PE-CH=CH or PE-COOH. Mechanism M2, described by PE-CH$_2$–CH* + H* → PE-CH=CH + H$_2$, requires an activation energy of $E_a \simeq 0.34$ eV to pick up a H atom from the (intra-chain) adjacent –CH$_2$– group, forming a H$_2$ molecule, and leaving a vinyl defect (PE-CH=CH) in its triplet state. The excited vinyl defect then relaxes into its ground state, emitting a photon of 3.1 eV, which is consistent with the experimental data of 2.89 eV.[12] Mechanism M3 (shown in Fig. 2) is thermodynamically more favorable. By reacting with an oxygen molecule,
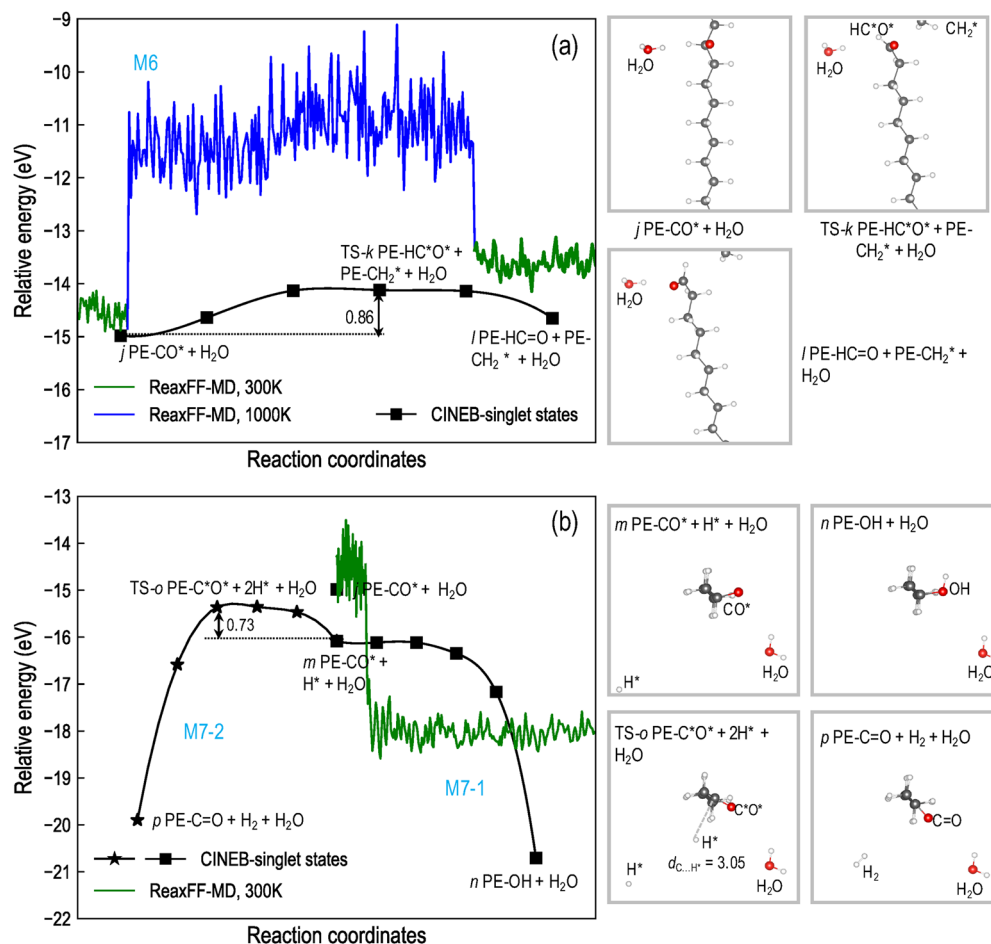
FIG. 4. (Left) CINEB reaction pathways (singlet in black) and ReaxFF-MD trajectories at 300 K (green) and 1000 K (blue) of M6 (a) and M7 (b), and (right) the structures of reactants, transition states, and products of M6 (a) and M7 (b). The isolated H_2O molecule is originated from mechanism M5.

hydroperoxide PE-COOH can be formed, releasing $\simeq 5$ eV. Mechanism M3 involves two substeps, including PE-CH* + O_2 → PE-COO* (M3-1) and PE-COO* + H* → PE-COOH (M3-2). The CINEB reaction pathways and the MD trajectories of mechanisms M3-1 and M3-2 shown in Fig. 2 reveal that these substeps are barrierless and can both happen at room temperatures, the typical condition of natural aging. Because hydroperoxide PE-COOH is $\simeq 2.23$ eV lower in energy than PE-COO* while the formation of this group is faster PE-COOH is likely to form, as detected in thermal-aged (and even initial) PE samples.[16]

C. M4 and M5: Intra- and inter-molecular reaction involving PE-COOH

The COOH group of PE-COOH can involve in either an intra-molecular (M4) or an inter-molecular decomposition (M5).[8,17] In mechanism M4, a H atom from the C atom of the COOH group reacts with the –OH group to form a H_2O molecule, while in mechanism M5, the H atom can come from any CH_2 units of the polymer. Detailed information of these two mechanisms is shown in Fig. 3.

Mechanism M4 produces PE-C=O and H_2O. The computed reaction pathways of M4 reveals that an activation energy of $E_a \simeq 0.39$ eV is required to dissociate the COOH group in its triplet state, forming the PE-CO$\cdots$OH transition

state and forming the PE-C=O product. If the reaction starts from the singlet state, the same transition state was found with $E_a \simeq 1.67$ eV, being closer to the experimental bond dissociation enthalpy of 2.02 eV measured for $(CH_3)_3COOH$ molecules.[23] The significant reduction of E_a is ascribed to the presence of triplet excitons that weaken the O–O bonds of the –COOH group. This argument is supported by the very low measured concentration of PE-COOH in UV[17] and electric field[18] aged PE, compared to thermal-aged PE.[17] In the former case, UV radiation and electric field can provide enough energy (1.5–4.0 eV)[17–19] to excite PE-COOH into its triplet state and accelerate the decomposition. The computed singlet-triplet gap of PE-C=O is $\simeq 3.15$ eV, being consistent with the measured electro-luminescence (EL) peak of 2.92 eV and chemi-luminescence (CL) peak of 3.0 eV.[19]

In mechanism M5, singlet PE-COOH decomposes through inter-molecular H-transfer, overcoming a barrier of $E_a \simeq 0.02$ eV to form the transition state PE-COOH$\cdots$H*, and ending at PE-CO* and H_2O as products. Our DFT and MD results show that mechanism M5 is significantly exothermic, releasing $\simeq 3.26$ eV.

Compared to mechanism M4, the electrostatic attraction between the OH and the H* radical in mechanism M5 makes the O–O bonds easier to break with a negligible barrier. Therefore, PE-COOH is likely to decompose
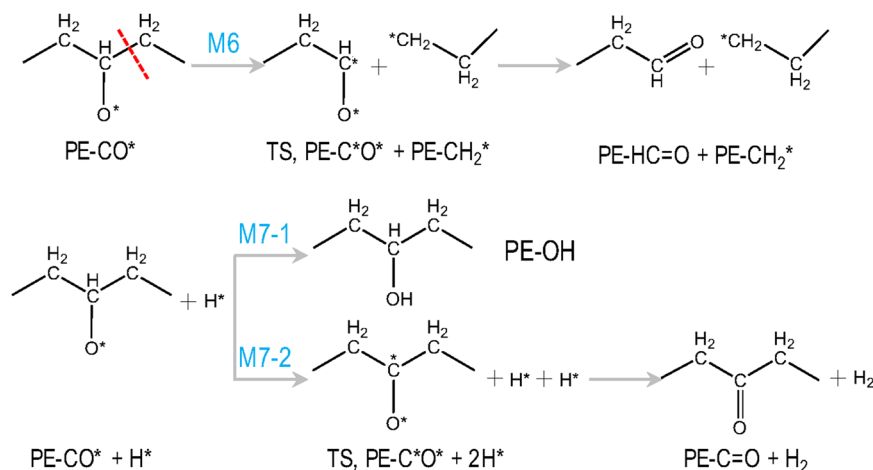
FIG. 5. Details of mechanisms M6 and M7, of which two sub-mechanisms M7-1 and M7-2 are shown.

by inter-molecular H-abstraction in the thermal-induced oxidation (at ~100 °C).[17] On the other hand, both mechanisms M4 and M5 can exist in electric- and photo-induced oxidation.[17,18]

D. M6 and M7: PE-HC=O, PE-OH, and PE-C=O formation

Two mechanisms (M6 and M7) can follow mechanism M5. When the external field is sufficient, the C–C bond between CO* and an adjacent CH$_2$ group can break, forming a PE-HC=O and a terminal radical PE-CH$_2^*$.[16,18,19] This mechanism, labeled by M6 and detailed in Figs. 4(a) and 5, requires an activation energy of $E_a \simeq 0.86$ eV. Our DFT and MD simulations indicate that mechanism M6 is endothermic, and thus the formation of PE-HC=O is favorable at high temperature-, electric field-, and UV radiation-induced oxidation processes.[16–18]

In mechanism M7, PE-CO* can react with a H* radical in two ways, forming either PE-OH (sub-mechanism M7-1) or PE-C=O (sub-mechanism M7-2). In M7-1, H* is captured by the O atom of the CO* radical, creating the –OH group of the product PE-OH. Our CINEB calculations and MD simulations at 300 K show that M7-1 is barrierless and can release up to 4.62 eV. Thus, this pathway is spontaneously exothermic and can occur naturally as supported by the observation of PE-OH in un-aged PE films.[17,18] In M7-2, the only H atom bonding to the C atom of the CO* radical is removed, forming a H$_2$ molecule with the H* radical (see Fig. 5). The transition state of this reaction (PE-C*O* + 2H*) defines the barrier of $\simeq$0.73 eV (or $\simeq$0.025 eV) when PE-CO* is in its singlet (or triplet) state. Two sub-mechanisms (M7-1 and M7-2) can occur simultaneously when the density of PE-CO* is high enough, creating both PE-OH and PE-C=O products.[17,18] This scenario involves two PE-CO* groups, and the activation energy E_a (of the sub-mechanism M7-2) depends on the distances between them. A maximum barrier of $\simeq$0.75 eV is required to form PE-C=O by inter-molecular reaction in the singlet state. Such barrier is much lower than that required by the intra-molecular reaction, i.e., 1.67 eV in mechanism M4. This suggests that the inter-molecular reaction may probably be the major pathway to form PE-C=O in the thermal-induced degradation.

Because the formation PE-OH (sub-mechanism M7-1) requires no energy, the concentration of this product is higher than those of PE-C=O and PE-HC=O in thermally aged PE samples.[17,18] However, in UV aged PE films, the concentration of PE-OH, PE-C=O, and PE-HC=O can be quite low while vinyl-type unsaturated bonds were observed at a higher density.[16,17] Presumably, UV radiation ranging from 1.5 to 4.10 eV can continuously break the first and second closest C–C bond to PE-C=O, requiring $E_a \simeq 0.86$ eV, i.e., Norrish reactions,[17] as shown in Fig. 4(a). As a result, short PE chains with C=O and C=CH$_2$ groups, and even acetone (CH$_3$)$_2$C=O molecules can be formed, as observed experimentally in PE samples.[16,17]

IV. SUMMARY

We have performed a systematic study of chemical defects formation in PE using a combination of density functional theory calculations and molecular dynamics simulations with ReaxFF classical potentials. The primary result of this work is that the proposed formation[3] of PE-CH* can trigger a chain of oxidation-induced chemical defects, including PE-CH=CH, PE-C=O, PE-OH, and PE-HC=O. The proposed microscopic mechanisms leading to these defects are validated against experimental data in multiple ways. Our findings provide a comprehensive connection among the available experiments in PE defects and aging. Our main conclusions are detailed as follows:

- The formations of PE-COO* (M3-1) and PE-COOH (M3-2) are barrierless and exothermic, and thus they can occur naturally. Hence, these are relevant to the natural aging process.
- The decomposition of PE-COOH via intra-molecular H-abstraction is a possible way to form PE-C=O, requiring 0.39 eV (or 1.67 eV) to break the O–O bond in the COOH group in the triplet (or singlet) state. The singlet decomposition may happen in photo-induced oxidation processes under UV radiation (1.5–4.1 eV). The (triplet) product PE-C=O can emit $\simeq$3.15 eV by relaxing into its singlet state, explaining the chemi-luminescence peak of 3.0 eV.[19]
- In the inter-molecular H-abstraction of PE-COOH, the barrier ($\simeq$0.02 eV) is negligible, suggesting that this

mechanism may be the predominant way to decompose PE-COOH in the thermal-induced oxidation (natural aging) process.

- From PE-CO* radicals, PE-HC=O and PE-CH$_2^*$ can be formed by breaking the C–C bond with a barrier of $\simeq$0.86 eV. This is followed by the formation of PE-CH$_3$ with no barrier and PE-CH=CH$_2$ with a small barrier (0.03 eV). PE-OH and PE-C=O can also be derived from PE-CO* with the involvement of a H* radical, crossing a barrier of 0, 0.73, or even as small as 0.007 eV. These stable products can be observed both in the thermal and UV aged PE samples.[16,17]

- Because PE-OH can be oxidized into PE-C=O with a small barrier when O atoms are present near the OH group (within 3.75 Å), PE-C=O and PE-HC=O are accumulated only in thermally aged PE samples.[17] In the presence of (high-energy) UV radiation, C–C scission of PE-C=O and PE-HC=O is dominant, resulting in a high concentration of unsaturated groups (e.g., PE-CH=CH$_2$), as observed experimentally.[17]

Overall, this work has laid the groundwork for an understanding of polymer degradation and breakdown. On the one hand, Fig. 1 can serve as the starting point for further exploration of polymer defect formation mechanisms. On the other hand, the electronic structure determined for the identified defects can be used within a phenomenological treatment of the carrier transport in polymer dielectrics, a promising pathway for reaching the large time and length scales of polymer degradation and breakdown. The mechanisms proposed here may also be studied under explicit electric field with nonadiabatic quantum molecular dynamics simulations[35] to better understand how electric field and temperature may combine and catalyze the formation of defects in polymers.

ACKNOWLEDGMENTS

[1] A. Peacock, *Handbook of Polyethylene: Structures: Properties, and Applications* (CRC Press, New York, 2000).

[2] T. D. Huan, S. Boggs, G. Teyssedre, C. Laurent, M. Cakmak, S. Kumar, and R. Ramprasad, Prog. Mater. Sci. **83**, 236 (2016).

[3] C. R. Bealing and R. Ramprasad, J. Chem. Phys. **139**, 174904 (2013).

[4] L. Chen, H. D. Tran, C. Wang, and R. Ramprasad, J. Chem. Phys. **143**, 124907 (2015).

[5] L. Chen, T. D. Huan, Y. C. Quintero, and R. Ramprasad, J. Mater. Sci. **51**, 506 (2016).

[6] L. Chen, T. D. Huan, and R. Ramprasad, Sci. Rep. **7**, 6128 (2017).

[7] D. M. Taylor, H. L. Gomes, A. E. Underhill, S. Edge, and P. I. Clemenson, J. Phys. D: Appl. Phys. **24**, 2032 (1991).

[8] L. A. Dissado and J. C. Fothergill, *Electrical Degradation and Breakdown in Polymers* (IET, London, UK, 1992).

[9] A. A. Mendes, A. M. Cunha, and C. A. Bernardo, Polym. Degrad. Stab. **96**, 1125 (2011).

[10] S. M. Mitroka, T. D. Smiley, J. M. Tanko, and A. M. Dietrich, Polym. Degrad. Stab. **98**, 1369 (2013).

[11] C. Wang, G. Pilania, S. Boggs, S. Kumar, C. Breneman, and R. Ramprasad, Polymer **55**, 979 (2014).

[12] C. Laurent, F. Massines, C. Mayoux, D. Ryder, and C. Olliff, in *IEEE Conference on Electrical Insulation and Dielectric Phenomena (CEIDP)* (IEEE, Virginia Beach, USA, 1995), pp. 93–96.

[13] A. M. Trozzolo and F. H. Winslow, Macromolecules **1**, 98 (1968).

[14] J. D. Peterson, S. Vyazovkin, and C. A. Wight, Macromol. Chem. Phys. **202**, 775 (2001).

[15] F. Gugumus, Polym. Degrad. Stab. **76**, 329 (2002).

[16] T. Corrales, F. Catalina, C. Peinado, N. Allen, and E. Fontan, J. Photochem. Photobiol. **147**, 213 (2002).

[17] M. Gardette, A. Perthue, J. L. Gardette, T. Janecska, E. Fldes, B. Puknszky, and S. Therias, Polym. Degrad. Stab. **98**, 2383 (2013).

[18] C. J. Mayoux, IEEE Trans. Electr. Insul. **EI-11**, 139 (1976).

[19] C. Laurent, G. Teyssedre, S. Le Roy, and F. Baudoin, IEEE Trans. Electr. Insul. **20**, 357 (2013).

[20] S. Le Roy, G. Teyssedre, and C. Laurent, IEEE Trans. Electr. Insul. **12**, 644 (2005).

[21] Y. Cao and S. Boggs, IEEE Trans. Electr. Insul. **12**, 690 (2005).

[22] F. H. Winslow, "Physical factors in polymer degradation and stabilization," in *Durability of Macromolecular Materials*, edited by R. K. Eby (American Chemical Society, Washington, DC, 1979), Chap. 2, pp. 11–27.

[23] S. J. Blanksby and G. B. Ellison, Acc. Chem. Res. **36**, 255 (2003).

[24] T. D. Huan, A. Mannodi-Kanakkithodi, C. Kim, V. Sharma, G. Pilania, and R. Ramprasad, Sci. Data **3**, 160012 (2016).

[25] S. Plimpton, J. Comput. Phys. **117**, 1 (1995).

[26] K. Chenoweth, S. Cheung, A. C. van Duin, W. A. Goddard, and E. M. Kober, J. Am. Chem. Soc. **127**, 7192 (2005).

[27] T. P. Senftle, S. Hong, M. M. Islam, S. B. Kylasa, Y. Zheng, Y. K. Shin, C. Junkermeier, R. Engel-Herbert, M. J. Janik, and H. M. Aktulga, npj Comput. Mater. **2**, 15011 (2016).

[28] G. Henkelman, B. P. Uberuaga, and H. Jnsson, J. Chem. Phys. **113**, 9901 (2000).

[29] G. Kresse, "*Ab initio* molekular dynamik für flüssige metalle," Ph.D. thesis, Technische Universität Wien, 1993.

[30] G. Kresse and J. Furthmüller, J. Comput. Mater. Sci. **6**, 15 (1996).

[31] G. Kresse and J. Furthmüller, Phys. Rev. B **54**, 11169 (1996).

[32] J. P. Perdew, K. Burke, and M. Ernzerhof, Phys. Rev. Lett. **77**, 3865 (1996).

[33] B. Baum, J. Appl. Polym. Sci. **2**, 281 (1959).

[34] N. Allen, J. Homer, J. McKellar, and D. Wood, J. Appl. Polym. Sci. **21**, 3147 (1977).

[35] F. Shimojo, S. Hattori, R. K. Kalia, M. Kunaseth, W. Mou, A. Nakano, K.-i. Nomura, S. Ohmura, P. Rajak, K. Shimamura, and P. Vashishta, J. Chem. Phys. **140**, 18A529 (2014).